# GRADIENT BEAM STEERING DEVICE BASED ON NEMATIC CELL WITH CONTINUOUS RAMP OF THE PHASE RETARDATION

Andrii B. Golovin, Sergij V. Shiyanovskii and Oleg D. Lavrentovich
Liquid Crystal Institute, Kent State University, Kent, Ohio, 44242-0001, USA
Email: odl@lci.kent.edu, Fax: (330)672-2796, Phone: (330)672-4844

*In order to develop a fine angular beam steering technique (milliradian and less), we propose a nematic liquid crystal cell with a continuous gradient of the refractive index. This continuous gradient is controlled by applying the driving voltage to non-patterned indium-tin oxide electrodes. We employed the dual-frequency nematic liquid crystal in the cell with high pretilt alignment. The experiments with dual-frequency nematic confirmed that non-patterned electrically controlled nematic cell with the continuous gradient of refractive index is capable of angular beam steering in the milliradian range.*

*Keywords: liquid crystal beam steering device, deflection angle, dual frequency nematic, gradient of the refractive index.*

## 1. Introduction

Optical scanning applications require optoelectronic systems, which provide the illumination of an object with a "flying" light spot of the laser beam. Usually the scanning process is executed by rotating mirrors, acousto-optic deflectors, mirrors with piezoelectric actuators or by gradient (electro-optic) prisms [1]. Rotating mirrors are composed of the mechanical attenuators with electro-motors or galvanometers, which adjust the angular position of the beam in the wide range (within radians). These mirrors provide a simple, rugged and low cost way of the scanners design. Acousto-optic deflectors are more precise devices, which use diffraction by acoustic waves. The scanning process, however, is accompanied by the loss of the light intensity. Mirrors between two piezoelectric actuators use deformations of piezoelectric plates and adjust angular position in the narrow range (within milliradians) [2]. Deformations of the mirror surface and mechanical oscillations, which accompany the scanning process, restrict the broad applications.
Another type of the laser scanners for the milliradians scanning angle range are beam steering devices based on a gradient of refractive index in an inhomogeneous optical medium, maintained, for example, by a laser beam that heats the sample [3]. The heating is slow, which limits the speed of scanning.

A more convenient way to design the beam steering device is to use the gradient of refractive index in a liquid crystal (LC) cell with electrically controlled birefringence. The beam deflects in the direction of a higher refractive index of the LC. The electrically controlled gradient of the refractive index is preferable, because it provides fast optical scanning with relatively low losses of the light intensity. In most cases, LC beam steering devices are based on a variation of the effective refractive index of extraordinary wave across the laser beam; see also Ref.[4] for a similar design in a polymeric material.

The Optical Phased Array (OPA) based on LC cell with N- striped electrodes of the applied voltages is the most advanced electrically controlled gradient prism design [5]. The pattern of stripped electrodes allows one to apply different voltages to different portions of the cell and thus to control the director configuration and the gradient of the refractive index across the laser beam, Fig.1a. The maximum deflection angle of the OPA is determined by the thickness *d* of the cell, optical anisotropy of the LC material $\Delta n = n_e - n_o$, where $n_e$ and $n_o$ are the extraordinary and ordinary refractive indices of the nematic LC, respectively, and the aperture *D*:

$$\delta_{\max} \approx \frac{\Delta L_{\max}}{D}, \tag{1}$$



Emerging Liquid Crystal Technologies, edited by Liang-Chy Chien
Proceedings of SPIE Vol.5741 (SPIE, Bellingham, WA, 2005)
0277-786X/05/$15 doi: 10.1117/12.588640

here $\Delta L_{\max} = \Delta n \cdot d$ is the maximum optical retardation achieved at one electrode. Because of the discrete character of the electrode pattern, the phase profile in such an OPA cannot be made absolutely smooth; the patterned electrodes also require a waveform generator with multiple channels.

In this report, we describe a LC beam steering device based on a continuous ramp of optical retardation shown in Fig.1b. Our design is based on a non-patterned electrode and thus leads to a smoother wavefront and reduces the number of independent channels of the waveform generator to two.


Fig.1. Quantized optical retardation profile in the standard OPA geometry with patterned electrodes (a) and ideal linear optical retardation profile in a LC cell with the voltage gradient (b); $\Delta L$ is optical retardation and X is longitudinal coordinate across the cell cross section.

### 2.1. Gradient Steerer Placed Between Two Dove Prisms.

The beam steering device with a continuous ramp of the optical retardation can be created by the continuous voltage gradient in the electrode material of finite resistance. In this way, we can use a nematic cell with one continuous non-patterned electrode at each bounding plate. The simplest scheme of the beam steering device based on the continuous ramp of the optical retardation is shown in Fig.2a. One of the plane electrodes, which are deposited onto the inner surfaces of glass substrates, is grounded from both sides. The second electrode is connected to the waveform generator from one side of the cell; the opposite side is grounded. The applied voltage creates the voltage gradient in the plane of the cell. Changing the amplitude of applied voltage, one can control the orientation of the nematic director in the cell [6, 7]. The monotonous voltage gradient thus result in the orientational gradient along the axis X in Fig.1, and thus in the monotonous gradient of the effective refractive index $n_o \le n_{eff} \le n_e$ for the wave polarized along the direction X. The created ramp of the optical retardation is always continuous, but it is not necessarily linear.

The switch in polarity of the gradient applied voltage at the driven electrode changes the director distribution across the nematic cell, which flips the tilt of the transmitting laser beam, Fig.2a. This switch of polarity can be implemented by rearranging the connections of the generator's hot wire and the ground, which are attached to the driven electrode.
One can improve the steering device by replacing the neutral electrode with a second driven electrode. This configuration can be employed in a dual-frequency nematic cell with high pretilt alignment, driven by two applied voltages at two different frequencies; for the low-frequency signal the LC behaves as a material with a positive dielectric anisotropy and for a high-frequency signal the dielectric anisotropy is negative. Figure 2b shows a schematic example, for a high-pretilt nematic cell filled with the dual frequency material MLC-2048 (available from EM Industries, Hawthorne NY), that has $\Delta\varepsilon$ =3.22 at frequency 1 kHz and $\Delta\varepsilon$ =-3.08 at 50 kHz (data correspond to the room temperature). This dual-frequency nematic cell should be driven using two waveforms of the applied voltage simultaneously. The low frequency applied voltage, at 1 kHz, causes the nematic state which is close to a homeotropic director configuration (perpendicular to the substrates) at one end of the cell. The high frequency applied voltage, at 50 kHz, favors a planar director orientation at the other end. Figure 3 shows the dependence of optical retardation vs. amplitude and frequency of applied voltage [8] for a flat uniform MLC-2048 cell. The beam deflecting performance of a LC cell with optical retardation ramp caused by the low amplitude of the applied voltage (depicted by dash line in Fig.3) might be approximately considered as propagation of the plane wave through the cell with an ideal linear ramp of


Proceedings of SPIE Vol.5741 (SPIE, Bellingham, WA, 2005)
0277-786X/05/$15 doi: 10.1117/12.588640

optical retardation. To reverse the ramp of the optical retardation, one can simply switch the frequencies of the two addressing voltage signals.

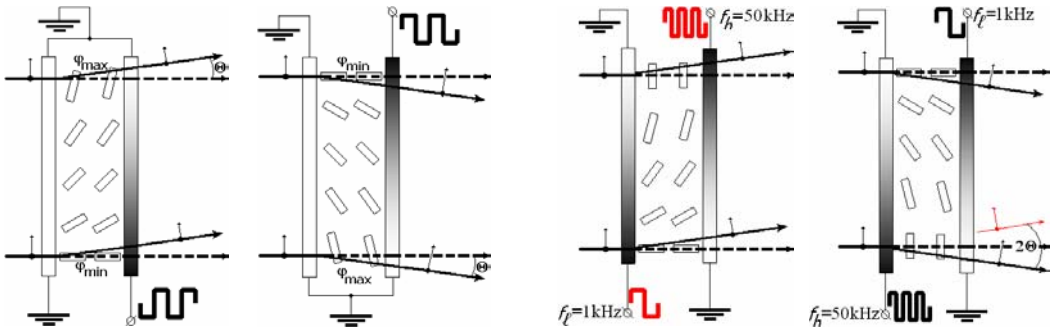


a) regular nematic cell b) dual frequency nematic cell

Fig.2. Optical design of the laser beam steerer using a nematic cell with continuous electrodes and driven by one (a) or two (b) waveforms of the applied voltage. Cylinders schematize the director inside the cell.

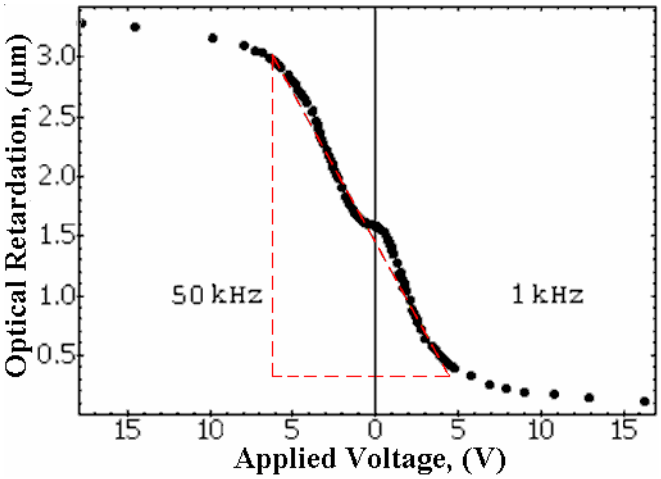


Fig.3. Optical retardation of MLC-2048 nematic cell vs. applied voltage. Parameters of the cell: thickness d=14.5 $\mu m$, temperature T=32°C, $\Delta\varepsilon(1kHz)$=2.5, $\Delta\varepsilon$ (50 kHz) =-1.2.

As follows from Eq. (1), the maximum deflection angle of the beam steering device based on gradient of refractive index is determined by the three parameters: the thickness of the cell, birefringence of the LC material and the optical aperture within which the gradient of refractive index is created. For example, one can obtain the deflection angle $\delta = 0.3$ mrad for He-Ne laser beam with *D*=0.01m deflected by MLC-2048 cell of thickness *d*=14.5 $\mu$ m; the LC birefringence is 0.2. One possible way to increase the deflection angle is to enlarge the thickness of the LC cell. We prepared the nematic cell between two glass Dove prisms as shown in Fig.4. The thickness of the cell was effectively enlarged as $d / \cos\alpha \approx 3.42d$, here $\alpha \approx 73^o$ is the incident angle of laser beam, Fig.4a.


Emerging Liquid Crystal Technologies, edited by Liang-Chy Chien
Proceedings of SPIE Vol.5741 (SPIE, Bellingham, WA, 2005)
0277-786X/05/$15 doi: 10.1117/12.588640

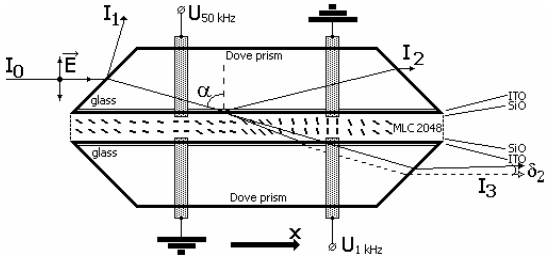


a

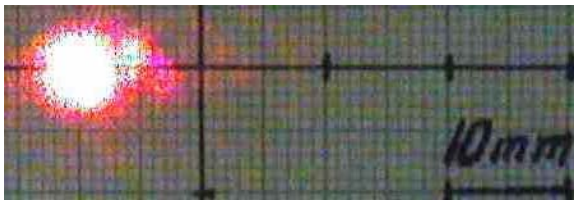


b) $\delta_1 \approx 2.5$ mrad ($U_{1kHz}$=8V; $U_{50kHz}$=8V)

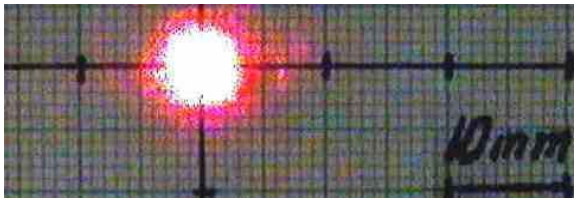


c) $\delta_0 = 0$

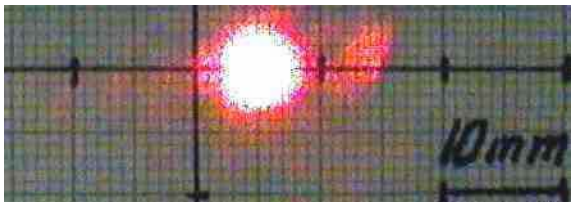


d) $\delta_2 \approx 1.25$ mrad, ($U_{1kHz}$=7.5V, $U_{50kHz}$=6V)

Fig.4. (a) Optical setup of He-Ne laser beam steering device based on 14.5μm thick dual-frequency nematic cell sandwiched between two Dove glass prisms: (b) and (d) are two extreme positions of the light spot; (c) initial position of the He-Ne laser spot that corresponds to the field-free state of the cell. The full deflection angle is $\delta_1 + \delta_2 \approx 3.75$ mrad**.**

In the experiment, we used the conducting electrodes made of thin Indium Tin Oxide (ITO) layers deposited onto the bottom sides of glass Dove prism. The characteristic resistance of ITO layer was around 300 $\Omega$/square. Each prism had two metallic electrodes to connect the waveform generator as shown in Fig.4a. The distance between two pair electrodes was 30 mm. To provide alignment layers for dual-frequency nematic MLC-2048, we used oblique deposition of thin SiO layers (≈20 nm) over the ITO electrodes. The cell was assembled in an anti-parallel fashion. The SiO layers yield a high pre-tilt angle $\alpha_b$, which the director $\mathbf{n}$ makes with the substrate. In what follows, we describe the cells with $\alpha_b \approx 45^o$, although the results were similar for a much broader range of angles $10^o \le \alpha_b \le 80^o$. The applied voltage aligns $\mathbf{n}$ perpendicularly to the cell plane (the homeotropic state), when the applied voltage frequency is $f_l < f_c$, and parallel to the plates when $f_h > f_c$, here $f_c$ is the so-called crossover frequency at which the material dielectric anisotropy is zero, $\Delta\varepsilon$=0. The high value of pretilt angle has several advantages. First, the dielectric torque of the applied field is maximized when the angle between the director and the field is about 45 degrees; second, there is no threshold for director reorientation; third, the high pre-tilt guaranties strong restoring surface torques that facilitate reorientation from both the homeotropic and the planar states. We used glass spacers to insure the uniform thickness of the cell gap.

The cell was filled in a vacuum chamber and then sealed by the epoxy glue. The cell was connected to the two channel waveform generator WFG-500 (FLC Electronics Inc., Sweden). To deflect the laser beam of He-Ne laser we simultaneously increased the amplitude of applied voltage of both carrier frequencies. Figures 4 b) and d) show the laser beam deflection as compared to the position of zero amplitude of applied voltage ($\delta = 0$) in Fig.4c. The maximum deflection angles were $\delta =$ -2.5/+1.25 mrad (depending on the polarity of the gradient). The intensity of the deflected


Proceedings of SPIE Vol.5741 (SPIE, Bellingham, WA, 2005)
0277-786X/05/$15 doi: 10.1117/12.588640

beam $I_3$ was rather high, 88% of the intensity of the incident beam $I_1$ even without antireflection layers on the input and output optical sides of Dove prisms.

### 2.2. Gradient Steerer Based on Nematic Cell Placed Between Dove Prism and Mirror.

There are many possible ways to modify the optical scheme of the gradient steerer to increase the deflection angle. For example, one could use a reflective setup, in which the dual-frequency nematic cell is sandwiched between a Dove prism and a mirror, Fig.5. In our experiment, we used an aluminum mirror covered by the transparent layers of insulator, ITO, and obliquely deposited SiO. The cell was assembled in the same way as the steerer placed between two Dove prisms.

Because of the mirror, the laser beam passes through the nematic cell twice, consequently the deflection angle is approximately two times larger. Figure 5b shows the voltage dependence of the deflection angle for the He-Ne laser beam, which we obtained by monotonously increasing the amplitude of applied voltage of both carrier frequencies. We observed beam distortions when higher voltages ($\geq$10V) were applied to the cell.

The challenge of this setup is to block the beam $I_2$ reflected by the bottom side of Dove prism, Fig.6. In our experiment the intensity of non-deflected beam $I_2$ was 4% of the intensity of the incident beam $I_0$; $I_2$ can be minimized by antireflection layers deposited on the bottom side of the Dove prism.

The maximum intensity of deflected beam $I_3$ strongly depends on the reflection coefficient of the multi-layer coated mirror. In our experiment we achieved $I_3$ equal to about 50% of the intensity $I_0$ of the incident beam.

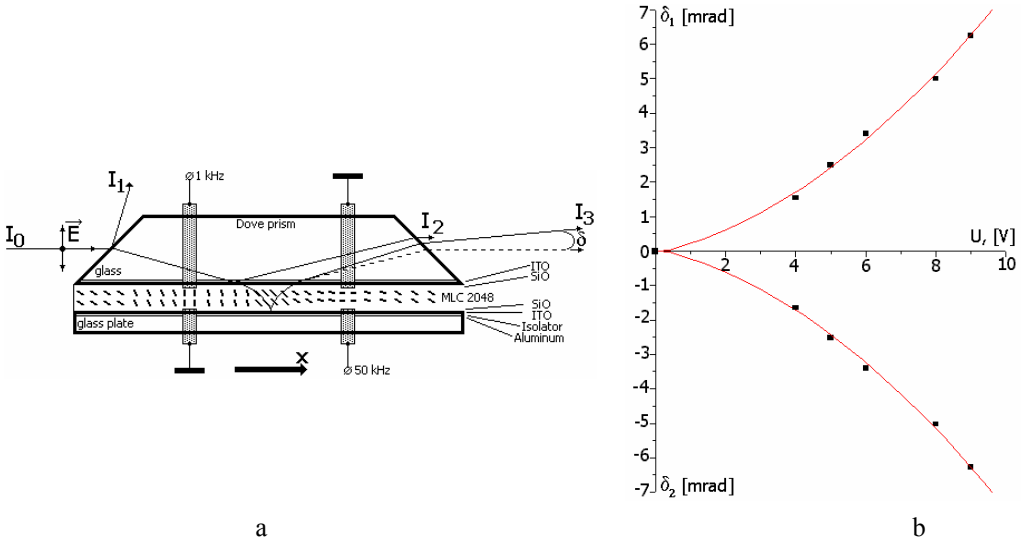


a b

Fig.5. The nematic cell with a gradient of the refractive index sandwiched between the Dove glass prism and the aluminum mirror (a), the deflection angle vs. amplitude of the applied voltage (b).

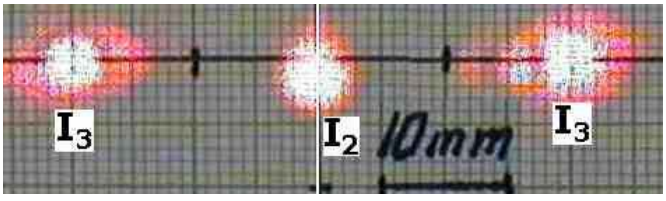


$\delta$ = -5 mrad, $\delta$ = 5 mrad,

$U_{1kHz}$=8 V, $U_{50kHz}$=6 V; $U_{50kHz}$=6 V, $U_{1kHz}$=8 V.

Fig.6. The laser beam spots in the plane of scanning: $I_2$ is the beam reflected by the bottom of the Dove prism, $I_3$ is the beam deflected by the dual-frequency nematic cell placed between the Dove prism and the mirror.


Emerging Liquid Crystal Technologies, edited by Liang-Chy Chien
Proceedings of SPIE Vol.5741 (SPIE, Bellingham, WA, 2005)
0277-786X/05/$15 doi: 10.1117/12.588640

### 2.3. Gradient Steerer with Compensation Loop

The magnitude of the steering angle is usually limited by nonlinear dependency of the optical retardation vs. apllied field when the voltage exceeds 10 V, Fig.3. The effect results effectively in convergent or divergent cylindrical lenses that distort the propagating beam, Fig.7.

The optical setup depicted in Fig.8 allows one to compensate the distortion of the laser beam by a loop trace containing a right angle glass prism. The laser beam enters the nematic cell two times from two opposite sides of the cell being turnined around in the loop optical scheme. The field vector of the initial laser beam $I_{in}$ is orthogonal to the vector of laser beam $I_\delta$ before second propagation through the nematic cell. Figure 8a shows an example of distortion compensation of the He-Ne laser beam: the initial round spot of the beam $I_{in}$, the distorted spot of the beam $I_\delta$ deflected during the first passage through the cell, and the compensated spot of the beam $I_{out,\Delta}$ passed through the LC cell twice; the maximum amplitude of the applied voltage was 17 V.

The steering angle of the device with the compensation loop is $\Delta \approx 2\delta$ as in the case of the nematic cell placed between the Dove prism and the mirror, but it is free of the "parasitic" beam $I_2$ reflected from the bottom side of the Dove prism.

An additional feature of the compensation loop depicted in Fig.8a is that the optical setup operates as a pair of lenses in an ordinary telescope in Fig.8b. The displacement of the right angle prism changes the divergence of output beam $I_{out,\Delta}$, so one would additionally collimate the deflected beam.

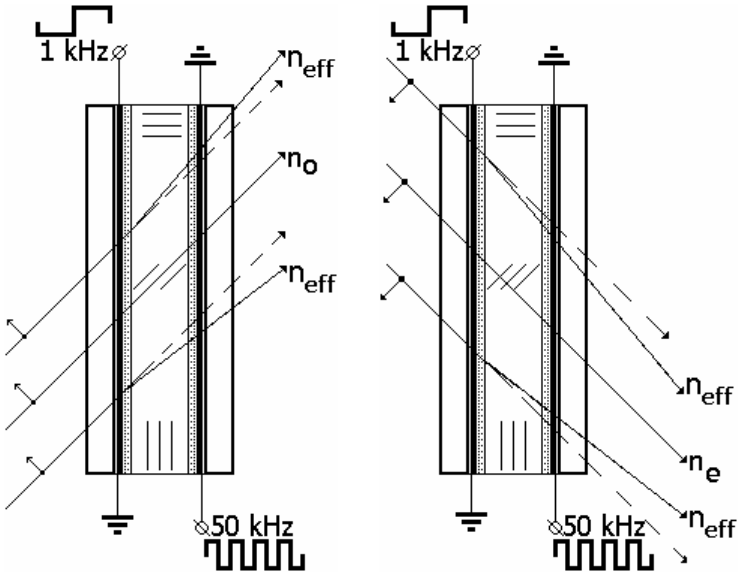


a b

Fig.7. Divergent (a) and convergent (b) cylindrical lenses leads to beam distortions.


Proceedings of SPIE Vol.5741 (SPIE, Bellingham, WA, 2005)
0277-786X/05/$15 doi: 10.1117/12.588640

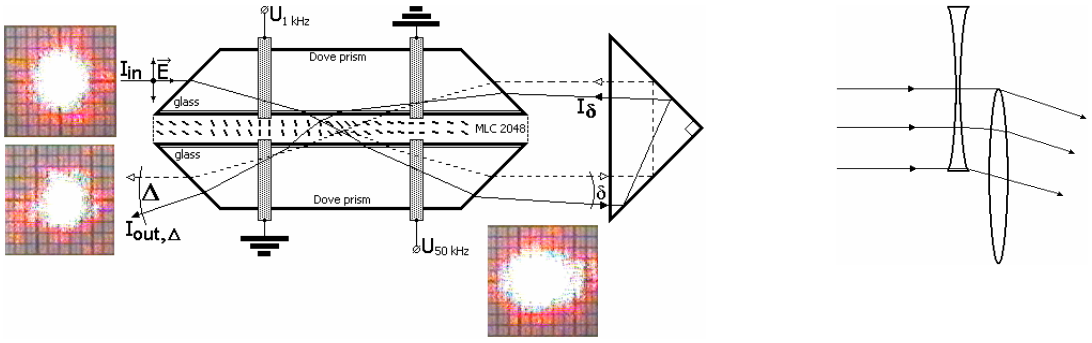


a b

Fig.8. Optical setup of the beam steerer with compensation loop (a), and an equivalent scheme of two lens telescope (b).

The nematic cell of continuous ramp of optical retardation can be used for waveguide applications. For example, we used two nematic cells to adjust the input and output angles of a laser beam propagating through a plane waveguide as shown in Fig.9. The dual frequency nematic was placed in the gaps between the right angle prisms and plane glass plate used as the waveguide. The alignment layers of SiO and ITO electrodes were deposited on the bottom sides of prisms and the upper side of the glass plate. We used right angle prisms in the mode of Dove prism as input and output couplers of the waveguide. The ITO electrode of the waveguide was grounded from two sides and the ITO electrodes of the prisms were connected to a waveform generator from one side and grounded from another. In our experiments, the assembled pair of the nematic cells was used to steer the output laser beam and to compensate the cylindrical lens distortion.
The steering efficiency of this optical design is the same as that of the beam steerer placed between two Dove prisms with the distortion compensating loop.

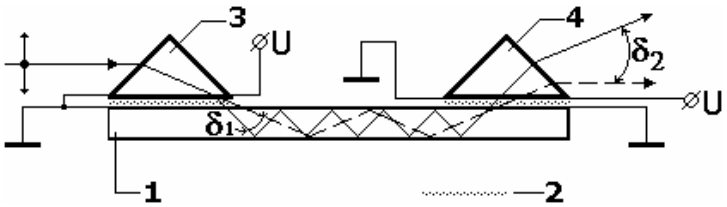


Fig.9. Optical setup of the plane waveguide with a pair of beam steering nematic cells: -1 is the plane glass waveguide, -2 is the nematic liquid crystal, -3 and -4 are the input and output right angle prisms, respectively, *U* is the applied voltage, $\delta_1$ and $\delta_2$ are the input and output steered angles.

## 3. Conclusion

We demonstrated an efficient beam steering by using a non-patterned electrically controlled dual-frequency nematic cell with a continuous phase retardation ramp. The steering angle continuously changes in the range of 10 mrad; the operating voltage is low, normally less that 10V. We demonstrate how to increase the steering angle and minimize the shape distortions of the propagating beam by using the Dove prisms and double passages of the beam through the nematic cell.

We thank Phil Bos for helpful discussions. Work was partially supported by DARPA Grant No.F33615-00-1-1681. The main results of this work have been presented in the report [9].

1. Handbook of Optics (Devises, Measurements, &Properties) vol. II, editor in chief: M. Bass, 1995.
2. 2. J.J. Shaffer, D.L. Fried. Appl. Opt., **9,** 933 (1970).
3. N.V. Tabiryan, S.R. Nersisyan. Appl. Phys. Lett., **84**, 5145 (2004).
4. L. Sun, J.H. Kim, C.H. Jang, D. An, X. Lu, Q. Zhou, J.M. Taboada, R.T. Chen, J.J. Maki, S. Tang, H. Zhang, W.H. Steier, C. Zhang, L.R. Dalton. Opt. Eng., **40**, 1217 (2001).
5. P.F. McManamon, T.A. Dorschner, L.J. Barnes. Opt. Eng., **32**, 2657 (1993);
   P. F. McManamon, T.A. Dorschner, D.L. Corkum, L. Friedman, D.S. Hobbs, M. Holz, S. Liberman, H.Q. Nguyen, D.P. Resler, R.C. Sharp, E.A. Watson. Proc. IEEE, **84**, 268 (1996).
6. G.D. Love, J.V. Major, A. Purvius. Opt. Lett., **19,** 1170 (1994).
7. S.A. Khan, N.A. Riza. Opt. Express, **12**, 868 (2004).
8. A.B. Golovin, S.V. Shiyanovskii, O.D. Lavrentovich. Appl. Phys. Lett., **83**, 3864 (2003).
9. Liquid Crystal Based Optical Phased Array for Steering Lasers, DARPA, Phase 1, Final Report, December 2001.


Proceedings of SPIE Vol.5741 (SPIE, Bellingham, WA, 2005)
0277-786X/05/$15 doi: 10.1117/12.588640